

TEM investigations in the PFN–PFW–PZN perovskite system

G. DRAŽIČ, M. TRONTELJ, D. KOLAR

"J. Stefan" Institute, University of Ljubljana, Jamova 39, 61000 Ljubljana, Slovenia

Using an analytical electron microscope, the distribution of phases and order-disorder phenomena in the $\text{Pb}(\text{Fe}_{1/2}\text{Nb}_{1/2})\text{O}_3$ – $\text{Pb}(\text{Fe}_{2/3}\text{W}_{1/3})\text{O}_3$ – $\text{Pb}(\text{Zn}_{1/3}\text{Nb}_{2/3})\text{O}_3$ (PFN–PFW–PZN) perovskite system were examined. It was found that after sintering the solid solution, small cubic pyrochlore particles with chemical composition close to $\text{Pb}(\text{Fe}_{0.28}\text{Zn}_{0.01}\text{Nb}_{0.50}\text{W}_{0.21})\text{O}_{3.4}$ and $a_0 = 1.05$ nm were present in the 0.8 mol % Pb_2WO_5 –0.2 mol % PbO liquid phase. In samples fired at 1000 °C, several 10 nm sized ordered areas with faint F spots in the selected-area electron diffraction pattern and $(h + \frac{1}{2}k + \frac{1}{2}l + \frac{1}{2})$ lattice fringes were found. Similar features were found in the PZN perovskite monocrystal, leading to the conclusion that local 1:1 ordering of cations (presumably Zn^{2+} and Nb^{5+}) in the PFN–PFW–PZN system caused partial decomposition of the perovskite phase at firing temperatures equal to or higher than 850 °C.

1. Introduction

The $\text{Pb}(\text{Fe}_{1/2}\text{Nb}_{1/2})\text{O}_3$ – $\text{Pb}(\text{Fe}_{2/3}\text{W}_{1/3})\text{O}_3$ – $\text{Pb}(\text{Zn}_{1/3}\text{Nb}_{2/3})\text{O}_3$ perovskite system (PFN–PFW–PZN) has been studied thoroughly [1–3] as a promising material for multilayer ceramic capacitors, with a low firing temperature, high dielectric constant and low dielectric losses.

In the present study, the results of TEM investigations of the PFN–PFW–PZN system are described. Distribution of phases, order-disorder phenomena and possible reasons for perovskite decomposition are discussed.

2. Experimental procedure

A solid solution with starting composition 0.48PFN–0.36PFW–0.16PZN (composition Y) with the addition of 0.1 at % Mn, was prepared from PbO , Fe_2O_3 , ZnO , Nb_2O_5 , WO_3 and $\text{Mn}(\text{CH}_3\text{COO})_2 \cdot 4\text{H}_2\text{O}$. All chemicals were reagent grade (p.a.). The homogenized mixture of oxides was pressed into compacts and calcined at 750 °C for 2 h. After milling in a zirconia mill, the powdered calcine was pressed into pellets which were sintered in air, at temperatures between 850 and 1000 °C.

For TEM investigations, the samples were ground, dimpled and thinned by ion bombardment (Ion Tech. Ltd ion mill) using argon ions at 4 kV and an incident angle of 15° to the specimen. Samples were examined at an operating voltage of 200 kV in a Jeol 2000 FX transmission electron microscope with EDX system (Link 10000 AN) attached.

Dielectric characteristics (dielectric constant and losses) as a function of temperature (in the range –30–120 °C) were measured on discs with silver

electrodes at opposite sides (Du Pont 7713, fired at 540 °C) using a 4192 A LF impedance analyser (Hewlett-Packard), connected to an HP 9825-T computer.

The degree of ordering was studied from X-ray diffraction (XRD) and selected-area electron diffraction (SAED) patterns [4, 5] and from the electrical measurements.

Yonezawa reported [1] that in the 0.48PFN–0.36PFW–0.16PZN system, in addition to the perovskite phase, traces of liquid phase, with a composition close to Pb_2WO_5 and a pyrochlore phase, presumably $\text{Pb}_3\text{Nb}_4\text{O}_{13}$, were present in samples sintered around 800 °C. He stated that the liquid phase enabled sintering, while the pyrochlore phase suppressed the grain growth of perovskite and consequently improved the bend strength of this material, compared to the PFN–PFW binary system.

We found in our previous work [6] that in the composition proposed by Yonezawa, the solid solution of perovskite formed at around 750 °C partly decomposes to zinc ferrite (ZnFe_2O_4) and 0.8 mol % Pb_2WO_5 –0.2 mol % PbO liquid phase at firing temperatures higher than or equal to 850 °C.

This was explained by the existence of some limiting zinc concentration in the perovskite structure for each firing condition. If this concentration was exceeded, Zn^{2+} ions were removed from the solid solution, forming zinc ferrite. To accommodate the excess of W^{6+} ions during ferrite formation, a liquid phase was formed, while Nb^{5+} ions remained in the perovskite structure, increasing the PFN content in the PFN–PFW–PZN system. With increasing sintering temperature, the volume fraction of ferrite and liquid phase also increased, and this influenced the dielectric properties of the ceramics as reported else where [7].

At prolonged firing times at temperatures higher than 850 °C, large regularly shaped pyrochlore grains were formed [6]. Based on results from diffusion-couple experiments, it was concluded that pyrochlore formation was due to high depletion of iron content, or a large excess of tungsten content in the system. In the case of prolonged firing times, PbO evaporated from the melt which thus became enriched in WO₃, leading to pyrochlore formation.

3. Results and discussion

3.1. Formation of the microstructure

0.8 mol % Pb₂WO₅–0.2 mol % PbO liquid phase (PW) and zinc ferrite (ZF) particles, found in samples with composition Y fired at 850, 910 and 1000 °C for 1 h, were present at triple points between perovskite (P) grains. Typical microstructure is presented in Fig. 1 where PW phase and a ZF particle in a sample fired at 910 °C for 1 h (sample 910/1) are shown. No liquid phase was detected at grain boundaries between two adjacent perovskite grains, suggesting that the PW phase does not form an interconnected skeleton, which was also confirmed by complex impedance spectroscopy [8].

On prolonged sintering of samples at 910 and 1000 °C, in addition to large pyrochlore (Py) grains [6], small pyrochlore particles (up to 100 nm) were found in the PW melt. Fig. 2 shows a transmission electron micrograph of a sample fired at 910 °C for 11 h. Comparing EDX spectra of small Py particles and the spectra of large Py grains, it was found that they had similar chemical composition, which was close to Pb(Fe_{0.28}Zn_{0.01}Nb_{0.5}W_{0.21})O_{3.4}. This pyrochlore phase is cubic with $a_0 = 1.05$ nm. Small Py particles formed in the liquid phase were probably seeds for large Py grains. The relatively large number of small Py particles in the PW melt indicated that most of them were generated during the cooling of the sample. Perhaps local chemical inhomogeneity of the

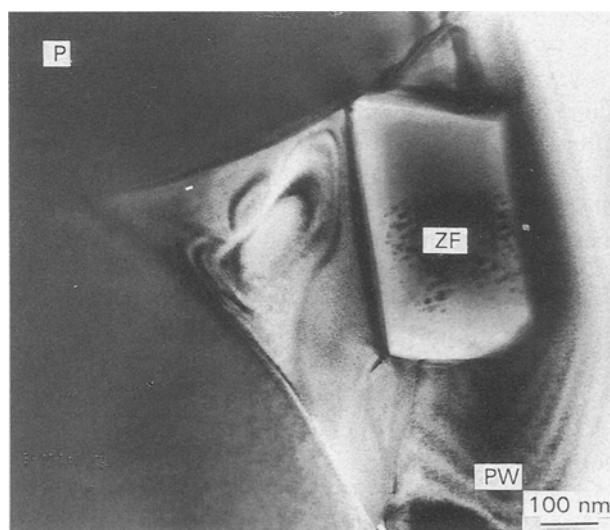


Figure 1 Transmission electron micrograph of a sample with starting composition Y fired at 910 °C, 1 h (ZF, zinc-ferrite; PW, liquid phase; P, perovskite).

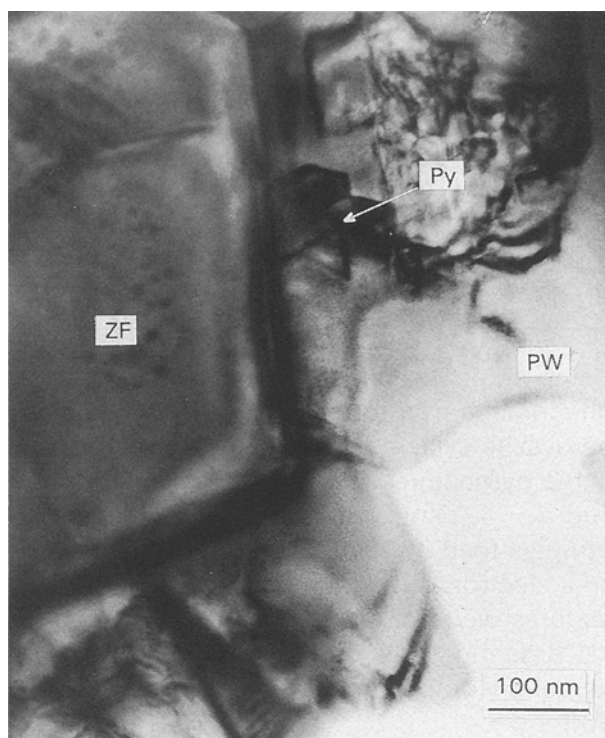


Figure 2 Transmission electron micrograph of a sample prepared at 910 °C, 11 h (Py, pyrochlore particles).

sample was the reason why only a few Py grains grew very quickly from the melt. Nevertheless, this exaggerated Py grain growth was in the $\langle 111 \rangle$ crystal directions and ended with large octahedrally shaped Py grains. Fig. 3 shows a high-resolution electron micrograph of Py particles in the PW melt of a sample fired at 910 °C for 58 h, and in Fig. 4 a scanning electron micrograph of a large, octahedral Py grain in the same sample is shown.

The assumption that during prolonged sintering PbO mostly evaporated from the liquid phase (PW) was confirmed by the observed fact that only this phase was volatile in contact with electron beam. Fig. 5 shows a high-resolution electron micrograph of the PW phase with many Moiré patterns which are the consequence of a crystalline PbO phase that has condensed on a thin foil of the investigated sample. The number and size of the areas with Moiré patterns grow with exposure time.

Exceptionally, in the prolonged sintering experiments, samples sintered at 850 °C did not display large Py grains. Although ZF particles were present in these samples, no liquid phase (PW) could be found by TEM investigation. In addition to perovskite and ferrite phases, small (50 nm) Py particles attached to the perovskite grain boundaries were present, as may be seen in Fig. 6.

An explanation for the formation of this microstructure could be that PW phase was formed at the beginning when the sample was heated to a temperature around 850 °C. Owing to the relatively low firing temperature, the amount of PW phase was very low and because of PbO evaporation, the melt gradually disappeared, and Py particles were formed. As there was insufficient melt present between the perovskite



Figure 3 High-resolution electron micrograph of Py phase in a sample prepared at 910 °C, 58 h.

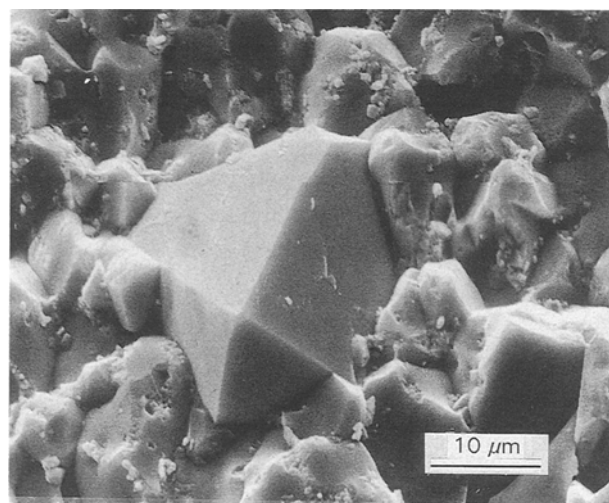


Figure 4 Scanning electron micrograph of a large Py grain in a sample prepared at 910 °C, 58 h.

grains, these particles could not grow into large octahedral grains.

Grain growth of the perovskite grains in this sample was affected by the disappearance of the PW melt and by the presence of Py precipitates. Table I gives the average intercept length of perovskite grains in samples prepared at different firing conditions. The grain-size differences between samples sintered for 1 and 11 h at firing temperatures of 850 and 910 °C could not be ascribed just to the different temperatures, but also to

TABLE I Average intercept length, \bar{l} , of perovskite grains in samples with starting composition Y sintered for different temperatures and times

sample (°C/h)	\bar{l} (μm)
850/1	1.0
850/11	1.3
910/1	1.3
910/11	3.0
1000/1	4.0
1000/15	10.0

different grain-growth mechanisms. While in the case of firing at 910 °C (and 1000 °C) sintering occurred in the presence of a substantial amount of liquid phase, in the case of firing at 850 °C for long times, solid-state sintering took place at a late stage of sintering.

These results explain why the optimal addition of PZN to the PFN–PFW binary system was 16 mol % under the firing conditions used by Yonezawa [1]. He found that for lower PZN additions, higher firing temperatures were essential to obtain an equal sintered density, and that at higher PZN additions the dielectric properties worsened.

Under the firing conditions (860–920 °C) used by Yonezawa, 16 % PZN produced an “optimum” quantity of the liquid phase (PW), promoting densification. During sintering, PbO partially evaporated from the melt and small particles of Py were formed

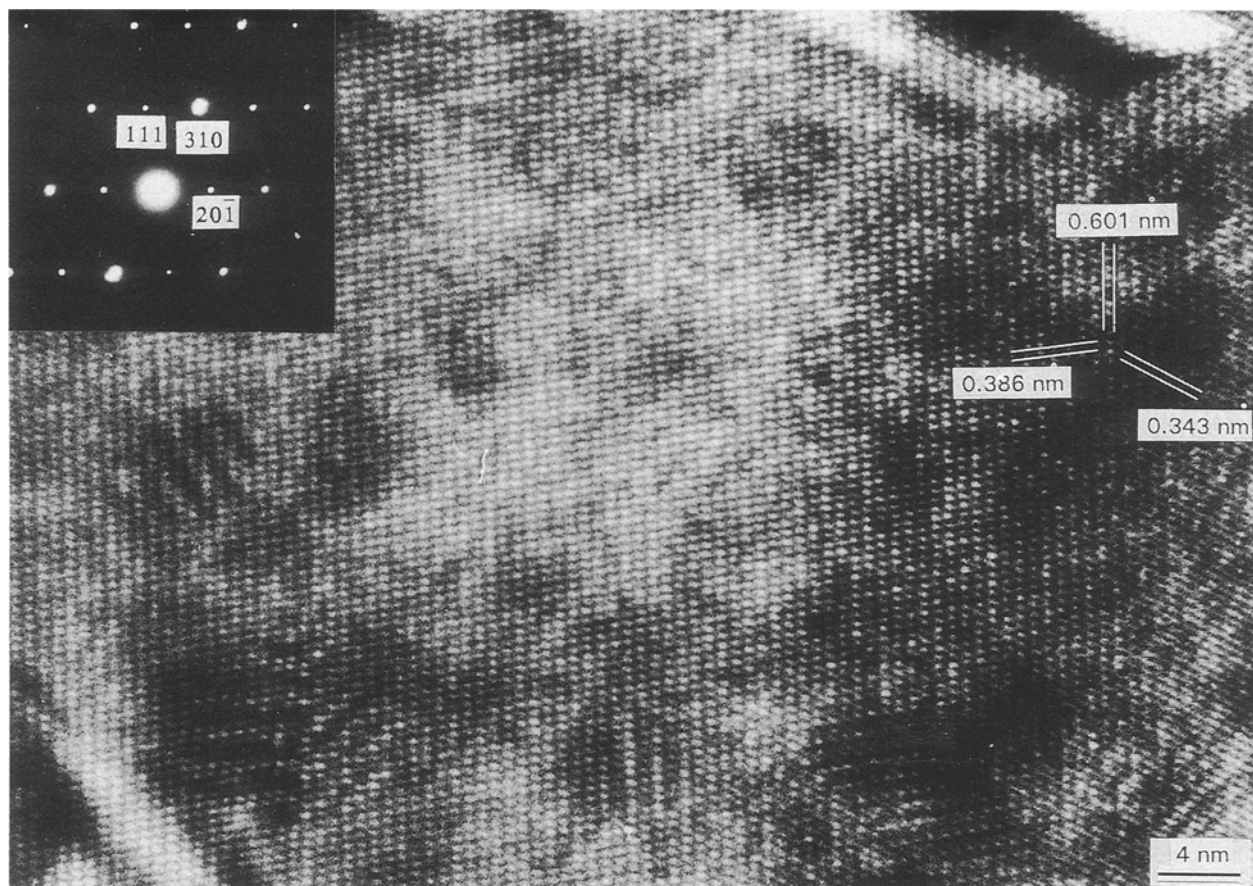


Figure 5 High-resolution electron micrograph of a PW phase in a sample prepared at 1000°C, 1 h.

between the perovskite grains, which enhanced the mechanical properties of the samples due to grain-growth suppression. If the amount of PZN was lower than 16 %, higher temperatures should be used for the same amount of PW melt. If the addition of PZN was higher, the amounts of PW and ZF phases were higher, lowering sintered densities and deteriorating dielectric properties.

3.2. Order-disorder phenomena in the PFN-PFW-PZN system

In many lead-based perovskite relaxors, ordering at B cation sites [9–11] was observed, influenced by the difference in B cation size and charge.

3.2.1. Electrical measurements

Equation 1 represents the empirical formula describing the dielectric constant of relaxors as a function of temperature [12] for the temperature region above the Curie temperature

$$\frac{1}{\varepsilon} - \frac{1}{\varepsilon_c} = C(T - T_c)^m \quad (1)$$

where T is the temperature, T_c the Curie temperature, ε the dielectric constant at temperature T , and ε_c is the dielectric constant at T_c . C is constant and m is a structure parameter with values between 1 and 2: $m = 2$ for complete disorder and $m = 1$ for complete order.

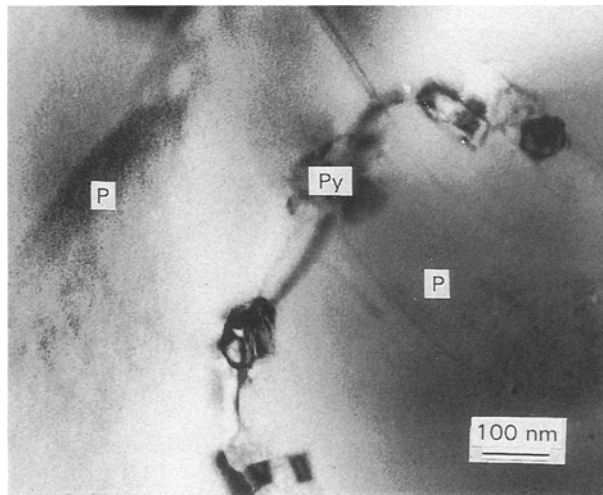


Figure 6 Transmission electron micrograph of a sample fired at 850°C, 11 h.

By plotting $\ln[(1/\varepsilon) - (1/\varepsilon_c)]$ versus $\ln(T - T_c)$, the parameter m was obtained for different samples with starting composition Y (Table II).

Another way to determine the degree of ordering is from the diffusive factor d , which represents the effective width of the Gauss distribution of local Curie temperatures in relaxor materials [13]. Factor d (°C) is calculated from Equation 2

$$\left(\frac{1}{\varepsilon} - \frac{1}{\varepsilon_c}\right) = \frac{1}{2\varepsilon_c d^2}(T - T_c)^2 + C \quad (2)$$

TABLE II Structure parameter, m , and diffusive factor, d , for samples fired at different temperatures for 1 h

Sample ($^{\circ}\text{C}/\text{h}$)	m	$d(^{\circ}\text{C})$
850/1	1.92	56
910/1	1.71	50
1000/1	1.50	37

C is usually close to 0, and the other symbols have the same meaning as in Equation 1. In Table II values of the factors d and m for samples with starting composition Y prepared under different firing conditions are listed. These results indicate that the degree of ordering depends on the temperature of firing; at higher temperatures the degree of ordering was higher.

The XRD patterns of the samples did not show any superstructure lines.

3.2.2. TEM studies of ordering

Using selected-area electron diffraction in TEM, faint F spots (at $(h + \frac{1}{2}k + \frac{1}{2}l + \frac{1}{2})$ positions) were found in the samples sintered at 1000°C for 1 h. Similar features were also observed in the sample first sintered at 850°C for 11 h and subsequently heated at 1000°C for 5 min and quenched in air. After such a treatment, additional decomposition of the perovskite phase took place, and high amounts of the PW phase were

detected at the triple points between perovskite grains (Fig. 7). In high-resolution electron micrographs of this sample, several 10 nm sized areas of perovskite grains with $(\frac{1}{2} \frac{1}{2} \frac{1}{2})$ lattice fringes were found. This is shown in Fig. 8, where the SAED pattern with weak F spots is also shown.

Other types of ordering, such as $(h + \frac{1}{2}k + \frac{1}{2}0)$ or $(h + \frac{1}{2}00)$ were not observed in these samples.

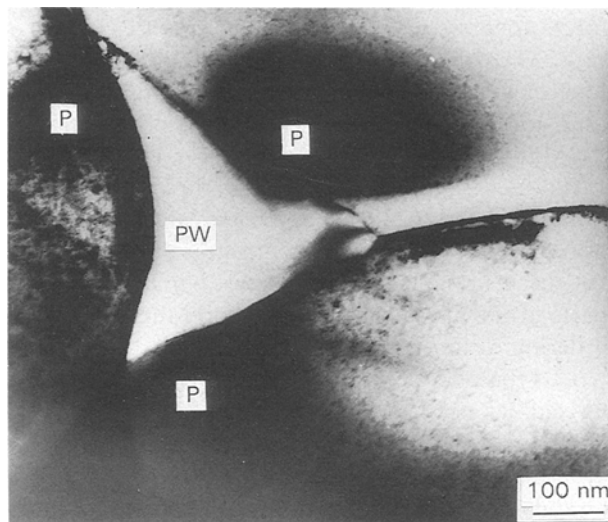


Figure 7 Transmission electron micrograph of a PW phase between P grains in a sample fired at 850°C 11 h, subsequently treated at 1000°C for 5 min and quenched in air.

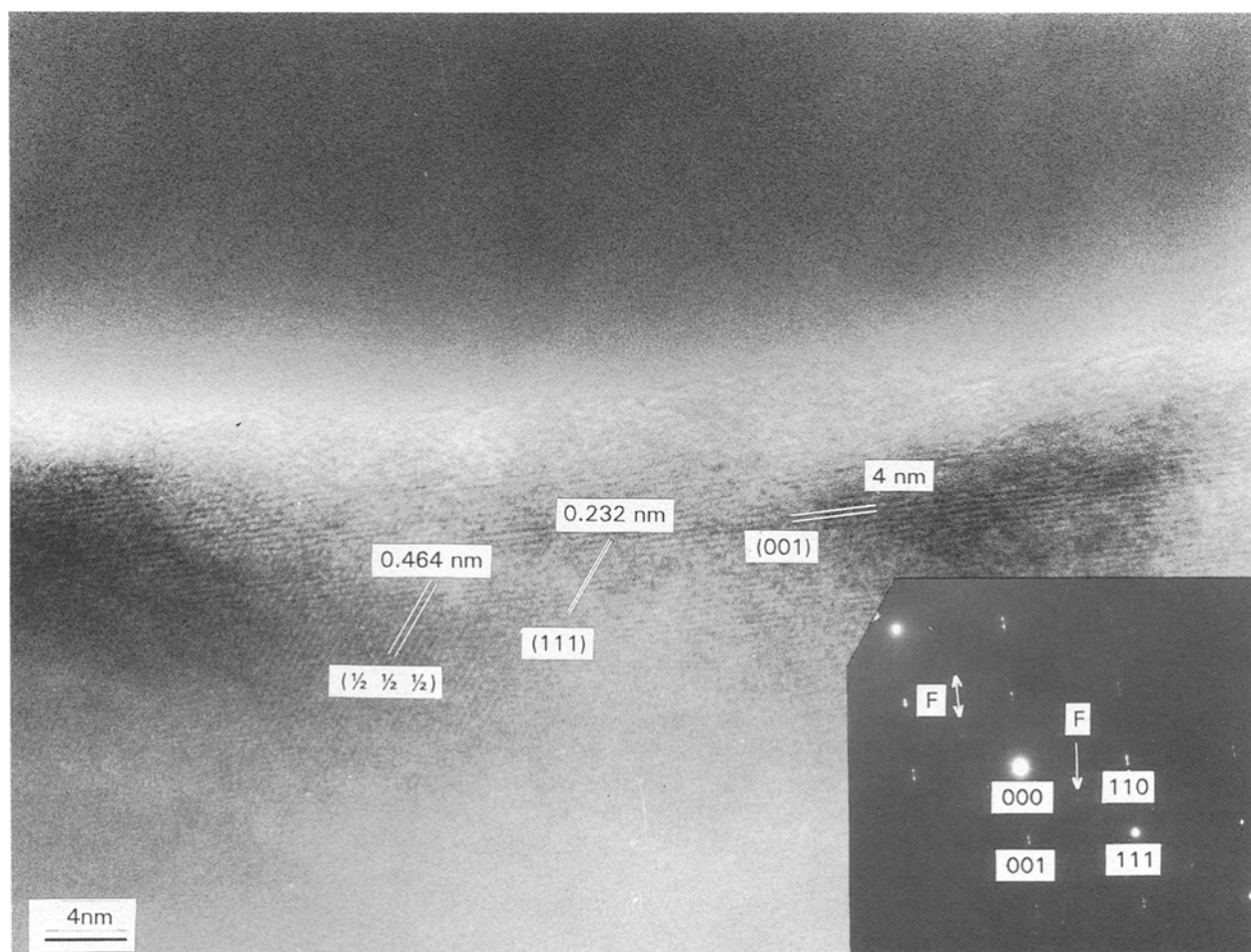


Figure 8 High-resolution electron micrograph of a perovskite phase in the same sample as in Fig. 7.

In samples sintered at lower temperatures or for longer times, we found no superstructural feature in the TEM study.

It was reported [14] that in some $\text{Pb}(\text{B}'_{1/3}\text{B}''_{2/3})\text{O}_3$ relaxor systems, small ordered areas can be observed where B' and B'' cations are ordered in a 1:1 molar ratio. These non-stoichiometric ordered areas are surrounded by a $\text{Pb}(\text{B}'')\text{O}_3^+$ -rich matrix which could easily decompose to pyrochlore. Owing to the non-stoichiometry in the ordered areas, strong electrostatic forces are present, prohibiting their growth. Growth of ordered areas is promoted by the addition of impurity ions of different valency, which compensate for the non-stoichiometry, as in the case of La^{3+} addition to $\text{Pb}(\text{Mg}_{1/3}\text{Nb}_{2/3})\text{O}_3$ relaxor material [14].

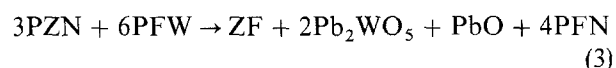
It was also reported [15] that in polycrystalline samples, ordering is faster and more extensive near the grain boundaries. The concentration of different lattice defects is higher in these areas than in the interior parts of the grains, and consequently the diffusion of ordering cations is faster.

1:1 type of ordering is specific for relaxors with a large difference in ionic-radii and valency numbers of B-site ions, as in the case of PZN [14]. To determine if ordering in PZN was indeed present, PZN monocrystals (in perovskite form) were prepared from a borate melt. In a TEM study of crushed pieces of PZN monocrystal, many ordered areas, several 10 nm in size, with faint F-spots in the SAED patterns were found, indicating the presence of 1:1 ordering. Lattice

fringes of $(\frac{1}{2}\frac{1}{2}\frac{1}{2})$ planes in PZN monocrystal are shown in Fig. 9.

The decomposition mechanism of a PZN perovskite monocrystal to ZnO and lead niobate during heat treatment in contact with a PFN–PFW binary system [6] could be related to such an unstable structure, due to 1:1 ordering of Zn^{2+} and Nb^{5+} ions.

Considering the similar dimensions of the ordered areas in a PZN monocrystal and in PFN–PFW–PZN samples with starting composition Y, and the fact that in PFN–PFW samples no ordering was detected, we suppose that also in PFN–PFW–PZN solid solution of perovskites, Zn^{2+} and Nb^{5+} ions form local ordered areas. We could assume that these unstable ordered areas also play an important role in the decomposition of PFN–PFW–PZN perovskite solid solution at temperatures higher than 750 °C. The decomposition products zinc ferrite and lead tungstenate (instead of zinc oxide and lead niobate) indicated that, in addition to PZN, in solid solution the PFW component also decomposed



where PZN is $\text{Pb}(\text{Zn}_{1/3}\text{Nb}_{2/3})\text{O}_3$, PFW is $\text{Pb}(\text{Fe}_{2/3}\text{W}_{1/3})\text{O}_3$, ZF is ZnFe_2O_4 and PFN is $\text{Pb}(\text{Fe}_{1/2}\text{Nb}_{1/2})\text{O}_3$; Pb_2WO_5 and PbO form PW liquid phase.

Based on all these considerations, we propose the following mechanism of PFN–PFW–PZN perovskite

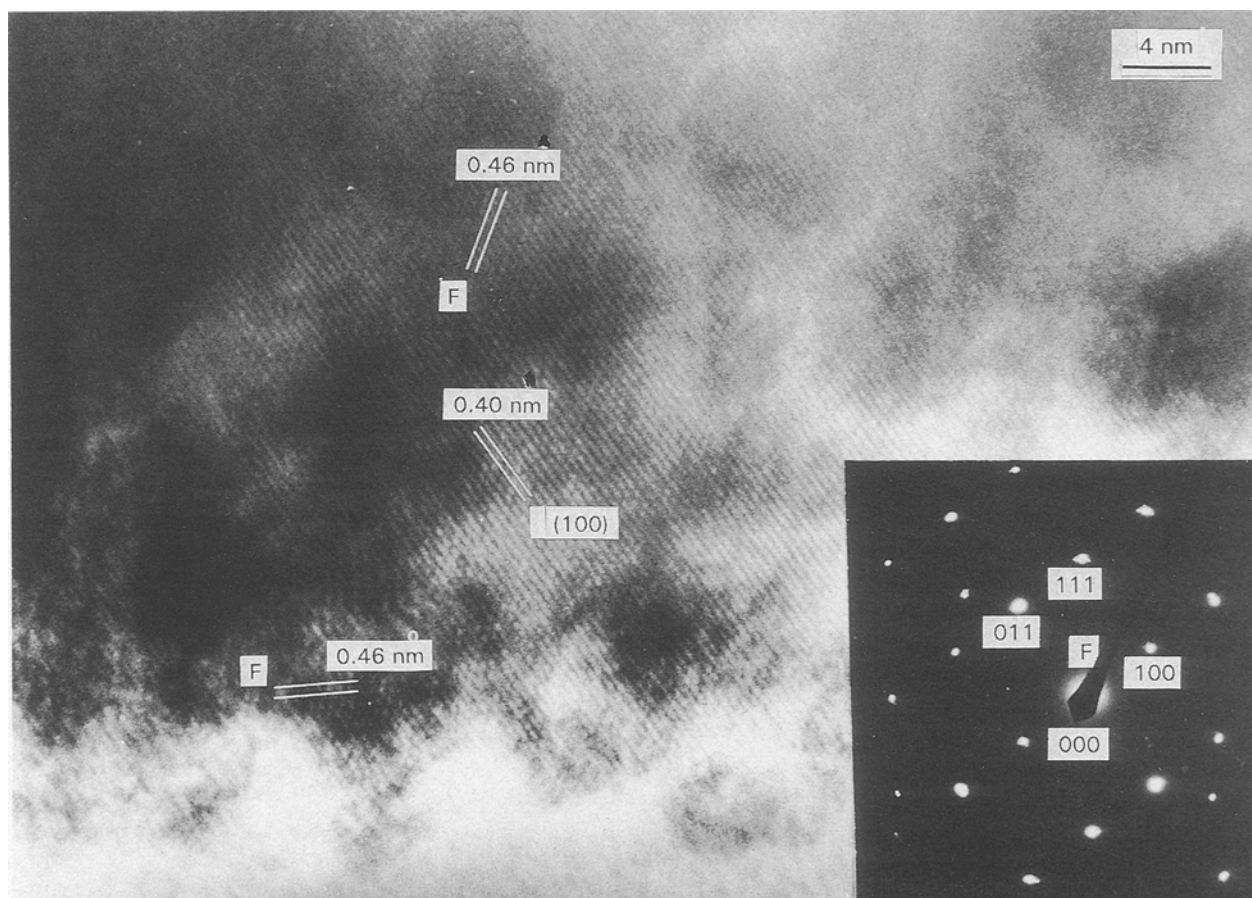


Figure 9 High-resolution electron micrograph of a perovskite phase in PZN monocrystal.

decomposition. During heating of samples with starting composition Y, almost pure perovskite phase is present at 750 °C. All the cations that occupy B sites in the perovskite lattice are randomly (not orderly) distributed on these sites. Owing to their large ionic radius and low valency number compared to other B site cations, Zn^{2+} ions represent sites of local distortion in the perovskite structure. At higher temperatures ($> 750^\circ\text{C}$) the diffusion rate of ions is higher and the possibilities for 1:1 ordered area formation is also higher, especially in the vicinity of grain boundaries.

On the basis of the observed fact that decomposition of perovskite phase does not take place inside the perovskite grains, we could conclude that either no ordered areas are present in the inner sides of the grains or that only ordered areas in the vicinity of grain boundaries are decomposed.

In the PFN–PFW–PZN system when decomposition of the perovskite structure due to local PZN ordering takes place, zinc ferrite (ZF) phase is formed as the most stable binary phase in this system. The PW melt is a by-product of such perovskite decomposition and ferrite formation, and the PFN content of the solid solution increased [6].

On raising the temperature, the diffusion of Zn^{2+} ions to the near-grain boundary areas (due to the depletion of zinc concentration) is enhanced, and the formation of ordered areas promoted. Subsequent decomposition of the perovskite lattice in the outer part of the grains produce more ZF and PW phase.

If the concentration of PZN component in the PFN–PFW–PZN system is lowered, then the probability of 1:1 ordering is smaller and higher temperatures are needed for perovskite lattice decomposition.

4. Conclusion

In samples with the composition 0.48PFN–0.36PFW–0.16PZN, fired at 1000 °C several 10 nm

sized ordered areas with faint F spots in SAED and $(h + \frac{1}{2}k + \frac{1}{2}l + \frac{1}{2})$ lattice fringes were found. Similar features were found in the PZN perovskite monocrystal, leading to the conclusion that local 1:1 ordering of cations (presumably Zn^{2+} and Nb^{5+}) in the PFN–PFW–PZN system caused partial decomposition of the perovskite phase to zinc ferrite and Pb_2WO_5 –PbO liquid phase at firing temperatures equal or higher than 850 °C.

Acknowledgement

The financial support of the Ministry of Science and Technology of the Republic of Slovenia is gratefully acknowledged.

References

1. M. YONEZAWA, *Am. Ceram. Soc. Bull.* **62** (1983) 1375.
2. M. KASSARIAN, R. E. NEWNHAM and J. V. BIGGERS, *ibid.* **64** (1985) 1245.
3. *Idem, ibid.* **64** (1985) 1108.
4. L. E. CROSS, *Ferroelectrics* **76** (1987) 241.
5. A. A. BOKOV, *ibid.* **90** (1989) 155.
6. G. DRAŽIČ, M. TRONTELJ and D. KOLAR, *J. Mater. Sci.* **25** (1990) 2590.
7. *Idem*, in "Proceedings of the 7th SIMCER", Bologna, 14–17 December 1988.
8. *Idem*, to be published.
9. C. G. F. STENGER, F. L. SCHOLTEN and A. J. BURGGRAFF, *Solid State Commun.* **32** (1979) 989.
10. A. BOKOV, I. P. RAEVSKII, O. I. PROKOPALO, E. G. FESENKO and V. G. SMOTRAKOV, *Ferroelectrics* **54** (1984) 241.
11. C. RANDALL, D. J. BARBER, P. GROVES and R. W. WHATMORE, *J. Mater. Sci.* **23** (1988) 3678.
12. R. CLARKE and J. C. BURFOOT, *Ferroelectrics* **8** (1974) 505.
13. B. ROLOV, *Fizika Tverdogo Tela* **6** (1964) 2128.
14. J. CHEN, H. M. CHAN and M. P. HARMER, *J. Am. Ceram. Soc.* **72** (1989) 539.
15. C. RANDALL, D. J. BARBER, R. W. WHATMORE and P. GROVES, *J. Mater. Sci.* **21** (1986) 4456.

Received 10 March 1992

and accepted 15 January 1993